ACS OMEGA

http://pubs.acs.org/journal/acsodf

Article

Plasma Functionalized Carbon Interfaces for Biosensor Application: Toward the Real-Time Detection of *Escherichia coli* O157:*H7*

Rahul Gangwar, Debjyoti Ray, Karri Trinadha Rao, Sajmina Khatun, Challapalli Subrahmanyam, Aravind Kumar Rengan, and Siva Rama Krishna Vanjari*

Cite This: *ACS Omega* 2022, 7, 21025−21034

Read Online

ACCESS | Metrics & More | Article Recommendations | Supporting Information

ABSTRACT: Nonthermal plasma, a nondestructive, fast, and highly reproducible surface functionalization technique, was used to introduce desired functional groups onto the surface of carbon powder. The primary benefit is that it is highly scalable, with a high throughput, making it easily adaptable to bulk production. The plasma functionalized carbon powder was later used to create highly specific and low-cost electrochemical biosensors. The functional groups on the carbon surface were confirmed using NH_3-temperature-programmed desorption (TPD) and X-ray photoelectron spectroscopy (XPS) analysis. In addition, for biosensing applications, a novel, cost-effective, robust, and scalable electrochemical sensor platform comprising in-house-fabricated carbon paste electrodes and a miniaturized E-cell was developed. Biotin−Streptavidin was chosen as a model ligand−analyte combination to demonstrate its applicability toward biosensor application, and then, the specific identification of the target *Escherchia coli* O157:*H7* was accomplished using an anti-*E. coli* O157:*H7* antibody-modified electrode. The proposed biosensing platform detected *E. coli* O157:*H7* in a broad linear range of $(1 \times 10^{-1}-1 \times 10^{6})$ CFU/mL, with a limit of detection (LOD) of 0.1 CFU/mL. In addition, the developed plasma functionalized carbon paste electrodes demonstrated high specificity for the target *E. coli* O157:*H7* spiked in pond water, making them ideal for real-time bacterial detection.

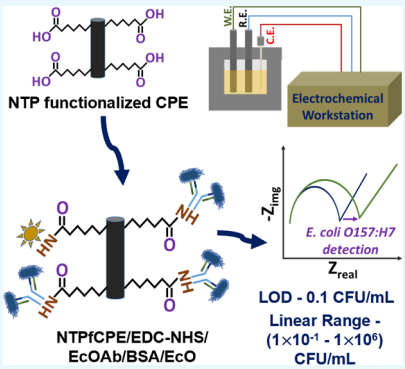

1. INTRODUCTION

Due to their cost-effectiveness, easy manipulation, and fast response, electrochemical biosensors have emerged with innovative designs to diagnose different diseases and detect various targeted biological agents.[1−4] In addition, they also offer the possibility of miniaturization for their use as point-of-care analysis, and the development of these sensors has been vastly improved using carbon materials.[4−6] The usage of different forms of carbon, such as graphite,[7] activated carbon,[8] graphene, carbon nanofibers/nanotubes,[9] fullerenes,[10] porous carbon,[11] and their composites,[12] is commonplace in electrochemical biosensors owing to their inherent advantages such as high chemical stability, excellent conductivity, superior mechanical strength, high surface-to-volume ratio, and biocompatibility. Furthermore, carbon materials can perform the dual role of a biorecognition element and a transduction element simultaneously.[13−15]

Bioreceptors are critical components that specifically bind with the target analyte of interest and govern the selectivity and sensitivity of the biosensor. The immobilization of such bioreceptors on top of the electrode surface is one of the critical steps in developing an ultrasensitive electrochemical sensor.[4−6,16] This is typically achieved by various surface functionalization techniques, which essentially bind the bioreceptor using noncovalent physical adsorption, electrostatic interactions, or covalent chemisorption. Furthermore, any surface functionalization method influences the electronical properties, signal transduction, and material interface. It is imperative to choose the right surface functionalization protocol to extract an optimum response from the sensor.[1,13−17] The throughput of this protocol governs the scalability of the sensor, an aspect that is key for commercialization.

Noncovalent interactions, in general, are simple and include the physical adsorption of the bioreceptors to the electrode surface but pose the limitation of nonspecific binding and long-term stability due to their weak interaction. In contrast, covalent interaction overcomes these limitations and provides stable attachment through covalent and specific cross-linking of the bioreceptors with the surface of the electrode. Among different covalent interactions, COOH terminated surfaces are frequently used in biosensor applications to bind bioreceptors through a covalent/ionic interaction. Self-assembled monolayers (SAMs) with COOH termination are broadly used for such purposes, but they are limited to specific substrates such

Received: March 25, 2022
Accepted: May 24, 2022
Published: June 6, 2022

as thiol for Au/Ag substrates and organosilane for silicon oxide substrates. Furthermore, such functionalization methods require hours to form SAMs and are likely to oxidize under certain conditions, making them unstable for prolonged use.[16,18]

The other modification methods involve the conventional oxidation of carbon materials through chemical treatment methods such as acid treatment. They involve a tedious process of multiple washing and filtration steps, followed by hot-air oven-drying. In contrast, the plasma-assisted formation of carboxylic groups is more stable and can also be used for different substrates. Plasma functionalization, which is a characteristic of generating active species under ambient conditions, possesses several advantages such as chemical interaction, stability, density, and coverage of the functionalized groups. In addition, this process is highly scalable, offering high throughput, and is readily amenable to bulk production for industrial applications.[13,16,17,19−21]

In general, plasma, the fourth state of matter, comprises partially or entirely ionized gas particles, such as electrons, ions, atoms, and molecules. The plasma technique involves thermal/nonthermal plasma and is regarded as a promising technique for changing the chemical surface properties of carbon materials because of the formation of active chemical species/functional groups on the surface. Due to its high-temperature operation, thermal plasma is a destructive technique and is not considered for such applications. In contrast, due to the low degree of ionization, nonthermal plasma (NTP) techniques have recently attracted significant attention toward the surface modification and engineering of different materials such as carbon, polymer, ceramic, and metallic surfaces without altering the bulk material properties. The surface functionalization of carbon materials through NTP can provide excellent reproducibility with remarkable specificity and sensitivity, unveiling different possibilities for biosensor applications. In this regard, one cost-effective NTP is dielectric barrier discharge (DBD), which uses AC voltage for operations due to a dielectric material present between electrodes, ensuring uniform discharge throughout the discharge volume.[15,20,22−24]

This work reports the usage of NTP as a nondestructive and scalable methodology for surface functionalization of carbon powders to generate carboxylic groups on the surface. Electrodes made of these functionalized carbon powders can be used to bind the bioreceptor and also transduce the interaction between the target analyte and the bioreceptor using well-known electroanalytical techniques. The focus is to maximize the carboxylic groups on the surface. To this extent, the carbon surface was functionalized using a DBD-plasma setup with different plasma treatments such as CO_2, H_2O, and CO_2 + H_2O treatments. Rigorous postcharacterizations such as NH_3-temperature-programmed desorption (TPD) analysis and X-ray photoelectron spectroscopy (XPS) revealed that CO_2 + H_2O gives a higher number of carboxylic groups on the surface. As a proof of concept, the proposed surface functionalization protocol is utilized to develop an ultrasensitive biosensor for *Escherichia coli O157:H7*.

Identifying pathogenic bacteria is a serious concern worldwide; swift and specific identification, therefore, becomes crucial to ensure the safety of food, the environment, and people. Among various pathogenic bacteria, *E. coli O157:H7* is considered one of the most dangerous foodborne pathogens causing life-threatening diseases such as hemorrhagic colitis, hemolytic-uremic syndrome, and severe gastrointestinal infections in some cases. Due to being simple, label-free, cost-effective, fast, sensitive, and specific, electrochemical sensors based on specific binding of the antigen and antibodies have emerged as excellent alternatives to traditional methods such as culture and colony-counting methods, enzyme-linked immunosorbent assays (ELISAs), surface-enhanced Raman scattering (SERS), colorimetric assays, and polymerase chain reaction (PCR) to identify pathogenic bacteria.[25−32] Recently, a few groups have already reported the identification of *E. coli O157:H7* with a limit of detection (LOD) of as low as 2−10 CFU/mL, but a lower limit of detection is still needed for bacterial analysis in food and clinical samples.[25,28,33,34]

Subsequently, novel and cost-effective carbon paste electrodes comprising plasma functionalized carbon were fabricated and used as working electrodes. In addition, a robust and cost-effective miniaturized E-cell was also engineered to reduce sample wastage and improve the electrochemical reversibility of the electrode. The physical picture of our fabricated miniaturized E-cell comprising the electrodes is attached as Figure S2 in the Supporting Information. The electrochemical experimentation of the detection of the well-known and straightforward Streptavidin with Biotin-modified electrodes was done in view of its applicability toward biosensors. Later, the swift and specific identification of the target *E. coli O157:H7* was accomplished using the bioelectrode having anti-*E. coli O157:H7* antibodies on its surface. Further, the selectivity and interference of the bioelectrode were studied using the nontarget *E. coli*, *Staphylococcus aureus*, and the mixture of both with the target *E. coli O157:H7*.

2. EXPERIMENTATION

2.1. Materials and Methods. In this work, graphite, poly(vinylidene difluoride) (PVDF), *N*-methyl-2-pyrrolidone (NMP), phosphate-buffered saline tablets (PBS (pH 7.4)), *N*-(3-dimethylaminopropyl)-*N*′-ethyl carbodiimide hydrochloride (EDC), *N*-hydroxy succinimide (NHS), and bovine serum albumin (BSA) were purchased from Sigma Aldrich. All of the chemicals obtained were of analytical grade and were used as received without any further purification. For all solutions prepared, deionized water (resistivity 18.2 MΩ/cm^{-1}) from the Millipore water purification system was also used for the cleaning and rinsing process. Brain heart infusion broth (BHI Broth) and Luria Bertani broth (Miller) were purchased from Sisco Research Laboratories (SRL) Pvt. Ltd. Mouse anti-*E. coli O157* antibody (E10) was obtained from The Native Antigen Company (U.K.), whereas *E. coli O157:H7* (ATCC 43888) were obtained from Microbiologics. *S. aureus* (MTCC 3160) were purchased from MTCC, and *E. coli* (ATCC 23724) were obtained from CCMB.

2.2. Instruments Used for Characterization and Detection. The DBD-plasma setup was used for different plasma treatments, including CO_2, H_2O, and CO_2 + H_2O treatments. NH_3-TPD analysis was performed to confirm the acidic sites present on the activated carbon using MicrotracBEL Corp., Japan, at a heating rate of 10 °C/min up to a maximum of 700 °C. Prior to the analysis, the samples were preheated at 150 °C for 1 h under a constant He flow to remove the physisorbed species. XPS was utilized to identify the elements present within the carbon or covering its surface along with their chemical states. All electrochemical measurements were performed using the CHI760E (CH Instruments, TX) electrochemical system as an electrochemical analyzer

https://doi.org/10.1021/acsomega.2c01802
ACS Omega 2022, 7, 21025−21034

comprising a miniaturized E-cell, a carbon-paste-coated working wire-electrode, a platinum (Pt) wire counter electrode, a carbon paste quasi-reference electrode (CPE), and 0.1 M PBS electrolyte containing a 2.5 mM redox couple ($[Fe(CN)_6]^{3-/4-}$).a

2.3. Protocol for Plasma Functionalization of Carbon. Prior to different plasma treatments, carbon powder was pretreated at 800 °C temperature for 4 h under an Ar flow (75 kg/cm^2) to confirm that there was no impurity on the surface of the carbon. The treated carbon was then stored in a controlled (airtight) environment to avoid moisture. Later, carbon was functionalized under different gaseous environments in a DBD-plasma reactor. The DBD-plasma setup is displayed in Figure 1 and has been discussed in detail in our earlier publication.[35]

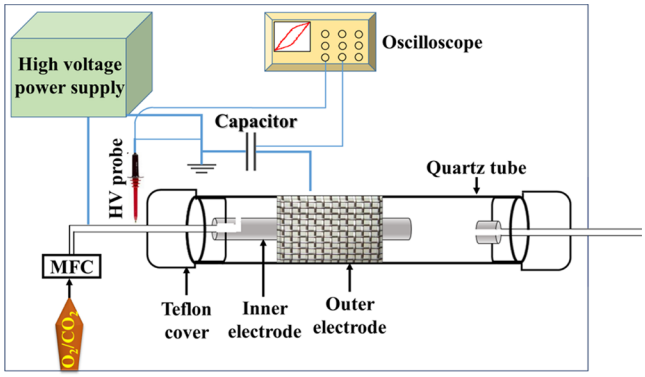

Figure 1. Schematic diagram of the experimental setup for plasma carbon treatment.

In brief, 5 g of activated carbon was placed in the discharge region of the DBD reactor, and N_2 gas was flown (30 mL/min) through a water bubble for H_2O treatment. Similarly, for CO_2 treatment, 30 mL/min pure CO_2 was introduced into the reactor, and 30 mL/min CO_2 was sent through a water bubble into the reactor for the combined treatment of CO_2 and H_2O. Later, after 10 mins, for each gaseous treatment, the plasma was operated at 20 kV for 4 h for surface functionalization. NH_3-TPD analysis was performed to confirm the acidic sites present on the activated carbon. Finally, the functionalized carbon was collected and tested for biosensing applications.

2.4. Protocol for Biosensing Studies. *2.4.1. Preparation of Bacterial Samples.* Our collaborator research group provided the bacterial cultures (*E. coli O157:H7*, *E. coli*, and *S. aureus*). All of the bacterial cultures consisting of *E. coli O157:H7*, *E. coli*, and *S. aureus* were cultured in BHI broth and incubated at 37 °C. Cells were then subinoculated in sterile BHI media and grown to an optical density (OD) of 0.1. The inoculum's turbidity was adjusted to standard 0.5 McFarland and diluted in saline, corresponding to bacterial cells around 1.5×10^8 CFU/mL (*E. coli and S. aureus*) and 1×10^8 CFU/mL (*E. coli O157:H7*). Further, different concentrations of *E. coli O157:H7* (1×10^1, 1×10^2, 1×10^3, 1×10^4, 1×10^5, 1×10^6, and 1×10^7 CFU/mL) and *E. coli and S. aureus* (1.5×10^1, 1.5×10^2, 1.5×10^3, 1.5×10^4, 1.5×10^5, 1.5×10^6, and 1.5×10^7 CFU/mL) to be tested were prepared in PBS by the process of serial dilution.

2.4.2. Fabrication of the Plasma Functionalized Carbon Paste Electrodes and Preparation of Bioelectrodes toward Streptavidin and E. coli O157:H7 Detection. In view of developing highly specific and cost-effective electrochemical sensors, plasma functionalized carbon interfaces were employed to fabricate the carbon paste electrodes. The protocol for the fabrication of electrodes has been discussed in our previous communication.[6] In brief, the in-house-developed carbon paste (made with the plasma functionalized carbon) was used to fabricate simple, novel, and cost-effective working wire-electrodes. The coating of carbon was done onto the surface of the stainless-steel wire with the help of a well-known and straightforward extrusion process followed by drying in a hot-air oven. The electrodes thus formed were stored and used as working and quasi-reference electrodes for electrochemical experimentation. The comparison of the various plasma functionalized CPEs was done through Biotin−Streptavidin, considering their affinity toward each other.

For the bioelectrode preparation, the well-known EDC-NHS chemistry (0.4 M, 4 h) was initially used to activate the carboxylic groups present on the plasma functionalized CPE (CO_2, H_2O, CO_2 + H_2O treated). The electrodes were then washed with DI water and were immersed overnight in a 100 ng/mL solution of Biotin to form a bioelectrode via amide bonding formed between the carboxylic groups and the amine groups present on the surface of the electrodes and in Biotin, respectively. Subsequently, the nonspecific sites of these surface-functionalized electrodes were blocked by BSA treatment and were then used as a bioelectrode to detect Streptavidin of different concentrations. The comparison of the various plasma functionalized CPEs through Biotin−Streptavidin detection studies is discussed in detail in the subsequent sections.

Further, as shown in Figure 2A, the preparation of a bioelectrode for *E. coli O157:H7* detection was also done similarly, wherein the COOH functional groups present in the CO_2 + H_2O plasma-treated carbon paste electrodes were first activated with EDC-NHS chemistry, followed by the immersion of these activated electrodes at 4 °C in the anti-*E. coli O157:H7* antibody of various concentrations (1, 5, and 10 μg/mL). The amine groups present in the antibody helped create an amide bond with the activated COOH terminated carbon paste electrodes. Finally, the nonspecific binding sites of these Ab immobilized electrodes were blocked by BSA treatment and were then used as a bioelectrode for *E. coli O157:H7* detection.

2.4.3. Protocol for Bacterial Detection, Interference, and Selectivity Studies. The electrochemical detection of *E. coli O157:H7* was done with the help of a three-electrode system comprising the prepared bioelectrode as a working electrode, CPE as a quasi-reference, and Pt wire as a counter electrode (Figure 2B,C). A total of 15 μL of each concentration of *E. coli O157:H7* was mixed in the miniaturized electrochemical cell containing 1.5 mL of the 2.5 mM redox couple ($[Fe(CN)_6]^{3-/4-}$) to obtain the final concentration ranges of 1×10^{-1}, 1×10^0, 1×10^1, 1×10^2, 1×10^3, 1×10^4, 1×10^5, and 1×10^6 CFU/mL. EIS analysis was done to attain charge transfer resistance (R_{ct}) after an incubation time of 30 min for each concentration of *E. coli O157:H7* to bind with the antibody present on the surface of the bioelectrode. At least three bioelectrodes were used for the EIS analysis of each measurement, and the results are discussed in the subsequent sections.

Additionally, the analytical performance of the biosensor was estimated by analyzing the selectivity and interference of the bioelectrode toward the different combinations of *E. coli*

https://doi.org/10.1021/acsomega.2c01802
ACS Omega 2022, 7, 21025−21034

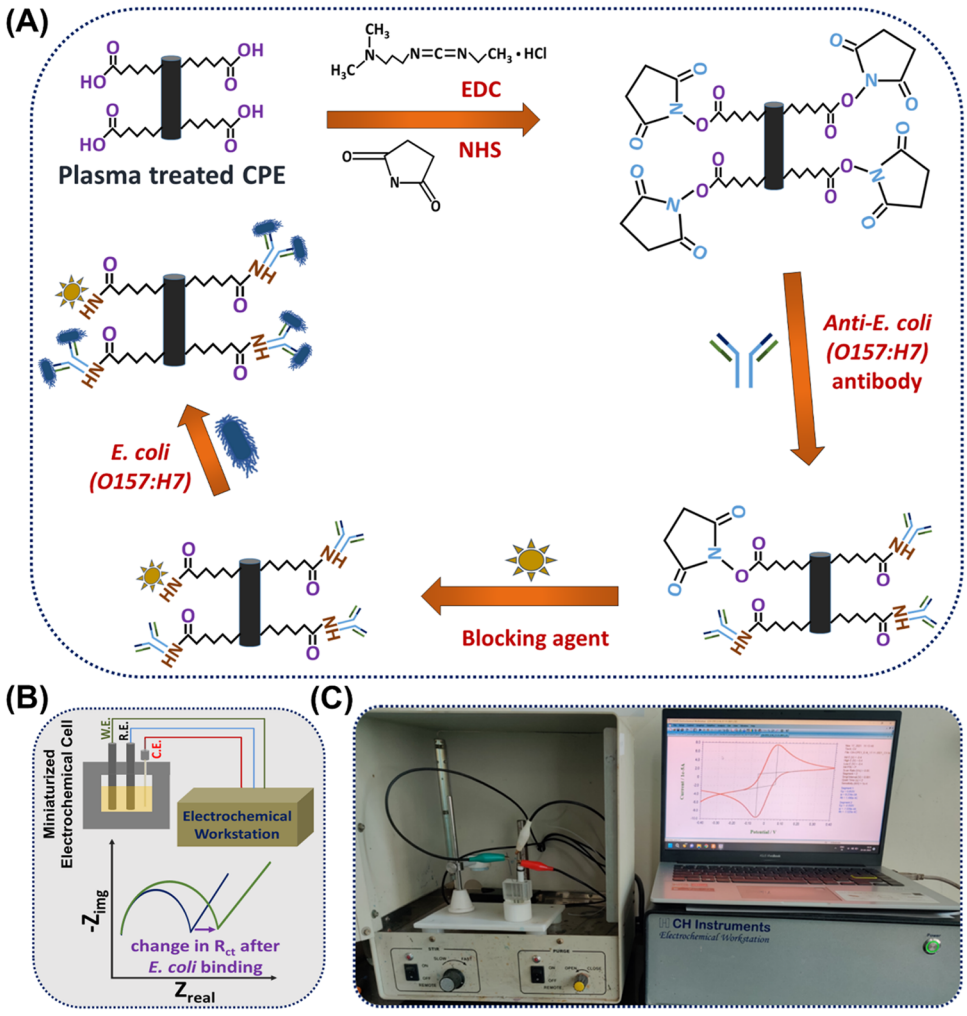

Figure 2. (A) Schematic showing the steps required to form a bioelectrode to detect *E. coli* O157:H7. (B) Demonstration of bacterial detection in a miniaturized E-cell. (C) Experimental setup with the miniaturized E-Cell.

O157:H7 with *E. coli* and *S. aureus* of various concentrations. The various combinations of all bacteria were selected in an equal ratio of 1:1 with concentrations of 1.5×10^0, 1.5×10^3, and 1.5×10^6 CFU/mL for E. coli and S. aureus and 1×10^0, 1×10^3, and 1×10^6 CFU/mL for *E. coli* O157:*H7*.

3. RESULTS AND DISCUSSIONS

3.1. Characterization Studies. For DBD-plasma treatment, the discharged power was calculated with the help of the Lissajous figure (Figure 3A), and it was found that a maximum of 1.1 W discharged power was utilized for the treatment. The aim of different plasma treatments on carbon powder was to create carboxylic groups onto the surface of the carbon to finally bind with an amine to generate an amide bond. All of these treatments helped create the carboxylic groups onto the surface of the carbon, but the number of carboxylic groups with each treatment was different, and the NH_3-TPD analysis revealed the same. Figure 3B describes the NH_3-TPD of different functionalized carbons. As shown in Table 1, CO_2 + H_2O-treated carbon showed the highest number of acidic sites, which is expected due to the simultaneous dissociation of acidic surface functional groups. The maximum weak acidic sites were observed in the case of only CO_2-treated carbon, which may be due to the moisture impurity present in the CO_2 source. The lowest acidic group was found with H_2O-treated carbon because of the least probability of COOH formation with OH radicals and solid carbon coupling.

Plasma functionalization under various plasma gases is known to produce varying amounts of acidic and basic groups on the surface. XPS analysis as shown in Figure 3C was hence utilized to analyze the surface chemistry of the plasma-treated carbon with different methods. Deconvolution of C 1s confirms the presence of graphitic carbon (284.5 eV); phenolic, alcohol, or ether groups (286.1 eV); carbonyl or quinone groups (287.4 eV); and carboxyl acidic groups (289.3 eV). Similarly, the O 1s peak position for oxygen was around 528 eV for raw carbon and 529 eV for plasma-treated carbon. In addition, it also shows that the plasma-treated carbon had a higher oxygen content (highest for CO_2 + H_2O-treated carbon) when compared to the untreated/raw carbon, which indicates that the different plasma treatments successfully grafted oxygen species onto the surface of the carbon. XPS analysis thus confirmed the successful incorporation of acidic groups through different plasma treatments (highest for CO_2 + H_2O-treated carbon), which are later utilized for biosensing applications. NH_3-TPD analysis, as discussed earlier, also confirmed the highest amount of acidic groups onto the surface of the CO_2 + H_2O-treated carbon.[18,36,37]

3.2. Streptavidin Detection Studies. For the application of plasma functionalized bioelectrodes toward electrochemical

https://doi.org/10.1021/acsomega.2c01802
ACS Omega 2022, 7, 21025−21034

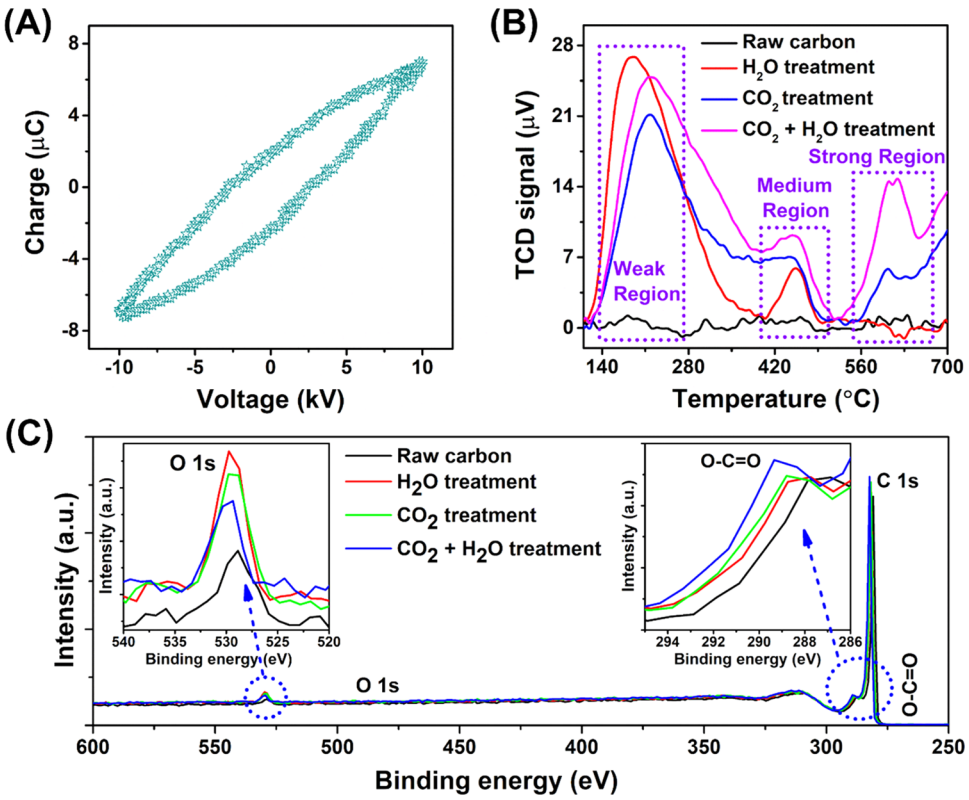

Figure 3. (A) Lissajous figure. (B) NH3-TPD for different functionalized carbons. (C) XPS analysis.

Table 1. Number of Acidic Sites Present on Each Carbon Sample

sample	weak (μmol/g)	medium (μmol/g)	strong (μmol/g)	total (μmol/g)
raw carbon	0	0	0	0
H_2O-treated carbon	7	1	0	8
CO_2-treated carbon	6	2	1	9
CO_2 + H_2O-treated carbon	8	3	3	14

biosensors, we need to have a significant number of carboxylic groups onto the surface of the carbon powder to have more numbers of receptors binding to the surface with the help of amide bonding. The electrochemical experimentation of a well-known and straightforward Biotin−Streptavidin detection was done in view of its applicability toward biosensors, as shown in Figure 4A. Biotin−Streptavidin, having a strong affinity toward each other, is used extensively as an ideal pair for validating the biosensing mechanism and so was an appropriate choice for biosensor applications. Moreover, these studies were performed to investigate the influence of carboxylic groups created onto the carbon surface with different functionalization techniques. To explain in detail, the Biotin-modified bioelectrodes formed using the plasma functionalized carbon (different treatments) were used to detect Streptavidin of different concentrations. Figure S1 in the Supporting Information shows the DPV response of Biotin-modified plasma-treated electrodes with different target Streptavidin concentrations. The results shown in Figure S1 display the reduction in peak current with the increase in the target

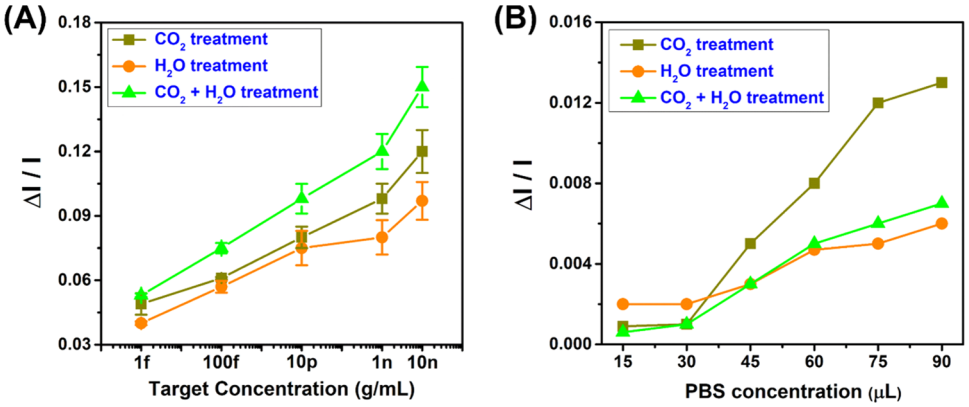

Figure 4. Biotin−Streptavidin detection. (A) Normalized current response obtained from DPV analysis for different concentrations of Streptavidin. (B) Normalized current response obtained from DPV analysis for different concentrations of PBS.

https://doi.org/10.1021/acsomega.2c01802
ACS Omega 2022, 7, 21025−21034

Streptavidin concentrations. The reduction in peak current was due to the successful binding of Streptavidin to Biotin, indicating the deterioration in reaction kinetics at the working electrode/electrolyte interface. Figure 4A and Table 2

Table 2. Biotin−Streptavidin Detection: Normalized Current Responses Obtained for Different Plasma-Treated Electrodes at Different Concentrations of Streptavidin

Streptavidin concentration	CO_2 treatment	H_2O treatment	CO_2 + H_2O treatment
1 fg/mL	0.049 ± 0.005	0.04 ± 0.0009	0.053 ± 0.0008
100 fg/mL	0.061 ± 0.0005	0.057 ± 0.0028	0.075 ± 0.0024
10 pg/mL	0.08 ± 0.005	0.075 ± 0.008	0.098 ± 0.0069
1 ng/mL	0.098 ± 0.007	0.08 ± 0.008	0.12 ± 0.0082
10 ng/mL	0.12 ± 0.01	0.097 ± 0.0088	0.15 ± 0.0094

correspond to the normalized current response obtained from DPV analysis (Figure S1) of each plasma-treated electrode, and the results displayed different current responses for the different plasma-treated carbon at different concentrations of Streptavidin. For a 10 ng/mL target Streptavidin concentration, the normalized current responses obtained for CO_2, H_2O, and CO_2 + H_2O plasma-treated carbon bioelectrodes were 0.12 ± 0.01, 0.097 ± 0.0088, and 0.15 ± 0.0094, respectively. The CO_2 + H_2O-treated carbon bioelectrode undoubtedly showed a significantly higher response compared to their counterparts. The different responses obtained for different plasma-treated carbon were due to the different numbers of carboxylic groups present on the surface of the electrodes. The higher number of carboxylic groups present on the CO_2 + H_2O-treated carbon paste electrode resulted in a higher response, whereas the response obtained with the CO_2- and H_2O-treated carbon paste electrode was comparatively low, suggesting a lower number of bindings with Streptavidin. The results obtained validate the initial findings and results obtained from XPS and NH_3-TPD analyses. The bioelectrodes accounted for a very low detection limit of 0.24 fg/mL, calculated using 3.3 σ/slope, where σ is the standard deviation of the blank response and slope = 0.011 was obtained from the linear fit of the calibration graph of Figure 4A (for the CO_2 + H_2O-treated electrode), showing the applicability of the plasma-treated carbon for biosensor application. Later, these electrodes were also subjected to control studies with PBS, and the results obtained from Figure 4B showed no significant response with different concentrations of PBS. The response received with PBS was almost negligible compared to the response obtained after Streptavidin binding to Biotin, offering an excellent selectivity of the bioelectrodes toward Streptavidin.

3.3. Bacterial Detection Studies. The results obtained from Biotin−Streptavidin showed a superior response toward CO_2 + H_2O-treated CPE, and therefore, the CO_2-H_2O-treated CPE was selected for *E. coli O:*157 detection. For this, the CPE was first fabricated from the CO_2 + H_2O-treated carbon, and later after DI water wash, these electrodes were stored and used to prepare a bioelectrode for *E. coli O:*157 detection. The schematic in Figure 2A shows the different steps required for a bioelectrode preparation to detect the different concentrations of *E. coli O:*157. The bioelectrodes formed were used for detecting various concentrations of *E. coli O:*157. DPV was used to optimize the incubation time and concentration of the anti-*E. coli O:*157 antibody, while EIS was used to detect various concentrations of *E. coli O:*157, followed by the interference and selectivity studies. Figure 5A,B shows the normalized current response obtained for the optimization studies of incubation time and concentration of the anti-*E. coli O:*157 antibody, respectively.

As shown in Figure 5A, for an antibody concentration of 5 μg/mL, the normalized current response obtained for various concentrations of *E. coli O:*157 was more prominent when the electrode was incubated for 45 min. It goes without saying that a higher incubation time led to more numbers of bindings when compared to its counterparts, but a larger incubation time also led to a larger detection time, and hence, the optimized incubation time of 30 min was selected, which was sufficient enough to bind and detect the *E. coli O:*157 with a good resolution. Later, the optimization studies of the anti-*E. coli O:*157 antibody concentration were done at an incubation time of 30 min, as shown in Figure 5B. The anti-*E. coli O:*157 antibody concentration of 10 μg/mL accounted for the higher response and sensitivity, significantly higher than the response obtained for 5 μg/mL at an incubation time of 45 min. It, therefore, was selected as an optimized concentration with an incubation of 30 min.

Figure 5C corresponds to the Nyquist plot obtained from electrochemical impedance spectroscopy of the EcOAbmCHCPE bioelectrode, before and after binding the target *E. coli O157:H7* at different concentrations of 1×10^{-1}−1×10^{6} CFU/mL. The results displayed in Figure 5C demonstrate an increment in charge transfer resistance (R_{ctn}) with every increasing target bacterial concentration, suggesting that the reaction kinetics at the bioelectrode/electrolyte interface is degrading with an increase in the target bacterial concentrations of *E. coli O157:H7*. This can be attributed to the fact that once the target bacterial concentrations of *E. coli O157:H7* are added to the electrolyte solution, they start binding with the immobilized anti-*E. coli O157:H7* antibody onto the surface of the bioelectrode.

The electrical behavior of the sensing mechanism is determined with the help of a modified Randle's circuit shown in the inset of Figure 5C, wherein the experimental values of the circuit elements (Table S2 in the Supporting Information) are obtained by fitting the obtained impedance data. In this circuit, the parameters R_s, R_{ct}, W, and CPE represent the solution resistance, the charge transfer resistance, the Warburg impedance, and the constant phase element indicating the behavior of a double-layer capacitance, respectively (refer to Section S1 in the Supporting Information for additional information). Figure 5D corresponds to the calibration curve where the normalized change in charge transfer resistance ($\Delta R_{ct}/R_{ct}$) is plotted at different target concentrations of *E. coli O157:H7*. Here, $\Delta R_{ct}/R_{ct}$ was calculated as $(R_{ctn} - R_{ct})/R_{ct}$, where R_{ct} and R_{ctn} ($n = -1$ to 6) represent the charge transfer resistance values of the bioelectrode without the target and the values obtained at different concentrations of target *E. coli O157:H7*, respectively. The error bars associated with each data point shown in Figure 5D represent the standard deviation ($N = 3$). A linear regression model was used to fit the curve shown in Figure 5D, which produced a linear equation (eq 1) with an adj. R-square value of 0.976.

$$y = 0.469 + 0.096\,x \quad (1)$$

Here, x represents the target concentrations of *E. coli O157:H7* and y is the dependent variable, i.e., $\Delta R_{ct}/R_{ct}$. The values 0.096

https://doi.org/10.1021/acsomega.2c01802
ACS Omega 2022, 7, 21025−21034

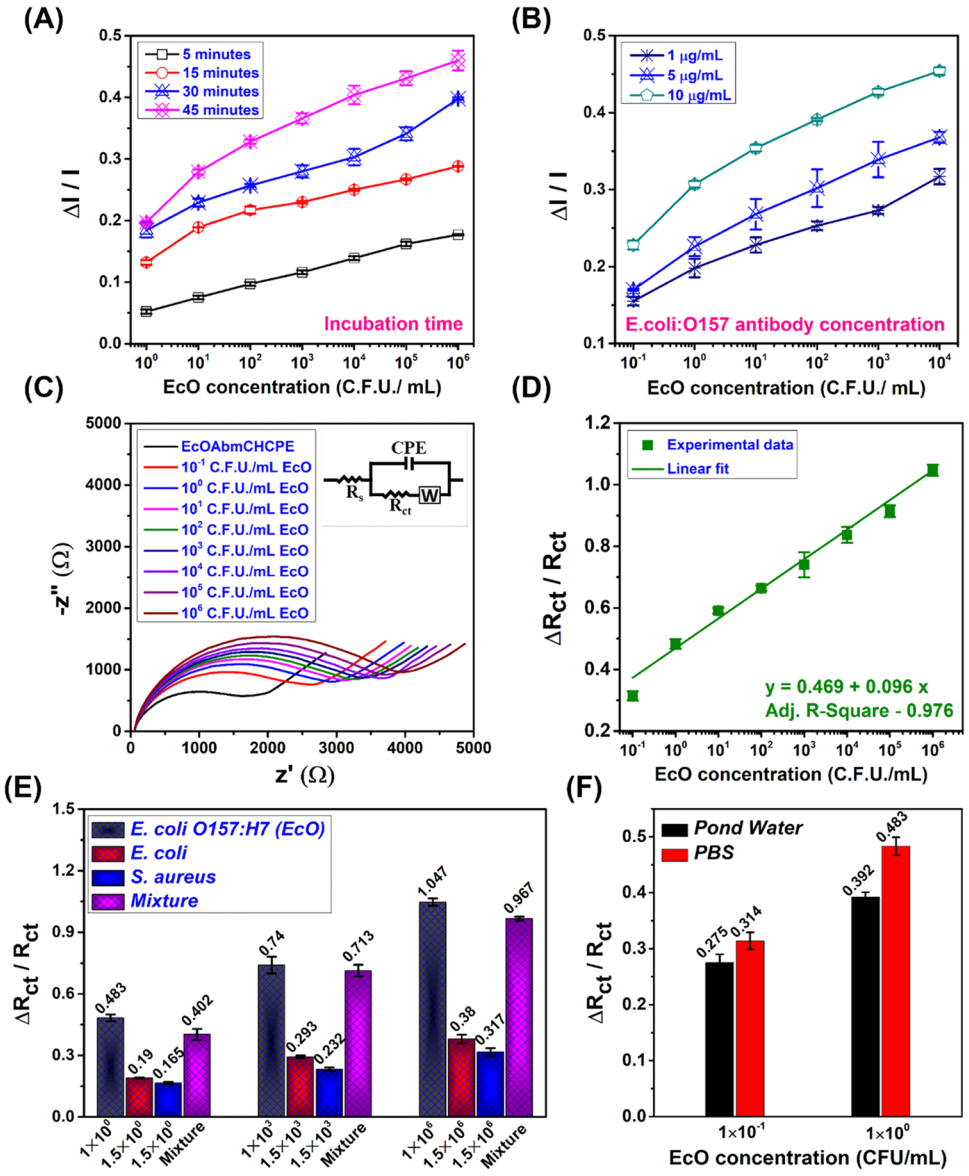

Figure 5. *E. coli* O157:H7 (EcO) detection, selectivity, and interference studies. (A) Normalized current response obtained from DPV analysis for various concentrations of *E. coli* O157:H7 at different incubation times (5 μg/mL anti-*E. coli* O157:H7 antibody concentration). (B) Normalized current response obtained from DPV analysis for various concentrations of *E. coli* O157:H7 at various concentrations of anti-*E. coli* O157:H7 antibody immobilized on a bioelectrode (incubation time of 30 min). (C) EIS analysis for various concentrations of *E. coli* O157:H7 detection (inset showing the modified Randle's circuit). (D) Calibration graph showing the normalized charge transfer resistance obtained from EIS analysis for various concentrations of *E. coli* O157:H7 (5 μg/mL anti-*E. coli* O157:H7 antibody concentration with an incubation time of 30 min). (E) Selectivity and interference studies. (F) Bar graph showing the normalized charge transfer resistance obtained from EIS analysis for various concentrations of *E. coli* O157:H7 spiked in PBS and pond water.

and 0.469 represent the slope and the intercept of the linear curve, respectively. The proposed sensing platform accounted for a sensitivity of 0.98 $((\Delta R_{ct}/R_{ct})/(\mathrm{CFU/mL}))/\mathrm{cm}^2$ with a wide linear detection range of 1×10^{-1}–1×10^{6} CFU/mL having an LOD of 0.1 CFU/mL. The limit of detection (LOD) and the sensitivity of the proposed biosensor were calculated using 3.3 σ/slope and slope/area, respectively, where slope = 0.096 was obtained from the linear fit of the calibration graph and σ is the standard deviation of the blank response. The LOD achieved with the proposed sensing platform is substantially low compared to that in the previous literature (Table S1 in the Supporting Information).

For point-of-care applications, the repeatability, interference, and selectivity studies of the proposed biosensing platform were also performed, and the same is shown as a bar graph in Figure 5E. The repeatability of the proposed sensing platform was investigated by successfully detecting different target *E. coli* O157:*H7* concentrations by taking three different electrodes. The results obtained were consistent throughout the experimentation, showing excellent repeatability and reliability of the proposed biosensing platform. An extensive study was done to understand the response of the bioelectrode at various concentrations of nontargeted *S. aureus*, *E. coli*, and their mixture with the target concentration (*E. coli* O157:*H7*). For this, the concentrations of *S. aureus* and *E. coli* were chosen in the range of 1.5×10^{0}, 1.5×10^{3}, and 1.5×10^{6} CFU/mL as well as 1×10^{0}, 1×10^{3}, and 1×10^{6} CFU/mL for the target *E. coli*. The mixture consists of all three bacteria in equal ratios

https://doi.org/10.1021/acsomega.2c01802
ACS Omega 2022, 7, 21025−21034

with the above-mentioned concentrations. The normalized change in charge transfer resistance is presented as a bar graph in Figure 5E. As illustrated in Figure 5E, for each concentration range, the normalized change in charge transfer resistance was the highest for the target *E. coli O157:H7* when compared to *S. aureus* and nontarget *E. coli*, alone, suggesting the excellent selectivity of the proposed platform. The dependency of the target *E. coli O157:H7* concentration can be seen in the mixture, implying that the proposed platform has a dominant response toward the target *E. coli*. The results indicated the superior response for *E. coli O157:H7*, suggesting its excellent selectivity and interference toward the interfering species, thus demonstrating its applicability toward swiftly identifying the target bacteria. In addition, we also demonstrated the applicability of the proposed biosensing platform toward real samples, and the same results are posted in Figure 5F. This was carried out by performing the experiments with bacterial samples prepared in pond water, and the results of the same were compared with the samples prepared in PBS. For this study, the concentrations of target *E. coli O157:H7* in PBS and pond water were chosen as 1×10^{-1} and 1×10^{0}, respectively, and the normalized change in charge transfer resistance obtained is presented as a bar graph in Figure 5F. As illustrated in Figure 5F, the normalized change in charge transfer resistance was the highest for the target *E. coli O157:H7* prepared in PBS when compared to its concentration prepared in pond water. The difference in the data values was probably due to the matrix effect present in pond water as it may contain several ions, bacteria, and other species. Although there was a difference between the absolute values of normalized change in charge transfer resistance, the difference was minimal, and the proposed biosensor could still identify the target *E. coli O157:H7* concentration in pond water with a dominant response. This suggested the excellent selectivity of the proposed platform, thus demonstrating its applicability toward identifying the target bacteria in real samples.

4. CONCLUSIONS

Nonthermal plasma functionalization is a straightforward, quick, and widely used surface modification technique for a variety of materials. Furthermore, it is a nondestructive and scalable surface functionalization methodology that is widely used to overcome the limitations of wet chemistry. Plasma functionalized carbon interfaces were used to create highly specific, low-cost electrochemical sensors. A DBD-plasma setup was used to functionalize the carbon surface, which included CO_2, H_2O, and CO_2 + H_2O plasma treatments. The presence of functional groups on the carbon surface was determined using NH_3-TPD and XPS analyses. Later, plasma-treated carbon was used to create novel and low-cost carbon paste electrodes. In addition, a robust and cost-effective miniaturized E-cell was built and engineered to reduce sample waste. Biotin−Streptavidin detection was performed due to its applicability to biosensors due to their strong affinity to each other. As a result of the superior response to the CO_2 + H_2O-treated bioelectrode, CO_2 + H_2O-treated CPEs modified with anti-*E. coli O157:H7* antibodies were later used to identify the target *E. coli O157:H7*. The proposed biosensing platform detected *E. coli O157:H7* with a wide linear detection range of 1×10^{-1}−1×10^{6} CFU/mL, accounting for an LOD and sensitivity of 0.1 CFU/mL and 0.98 $((\Delta R_{ct}/R_{ct})/(\text{CFU/mL}))/\text{cm}^2$, respectively. Furthermore, the bioelectrode's selectivity and interference were investigated using nontargeted *E. coli*, *S. aureus*, and a mixture of both with the target *E. coli O157:H7*. The superior response for *E. coli O157:H7* in the mixture of interfering species suggested its excellent selectivity and interference, along with excellent repeatability and reliability. In addition, the applicability of the proposed biosensing platform toward real samples (*E. coli O157:H7* spiked in pond water) was also demonstrated. The results suggested high specificity for the target *E. coli O157:H7*, making this methodology suitable for real-time bacterial detection.

■ ASSOCIATED CONTENT

Supporting Information

The Supporting Information is available free of charge at https://pubs.acs.org/doi/10.1021/acsomega.2c01802.

Figure S1, DPV response of Streptavidin detection; Figure S2, designed electrochemical sensor platform; Section S1, additional information about EIS and its corresponding Figure S3; comparison Table S1 of antibody immobilized electrochemical biosensors for detection of *E. coli O157:H7*; Table S2, experimental values obtained after fitting EIS data for different circuit elements corresponding to Figure 5C in the main manuscript (PDF)

■ AUTHOR INFORMATION

Corresponding Author

Siva Rama Krishna Vanjari − *Department of Electrical Engineering, Indian Institute of Technology Hyderabad, Hyderabad 502284, India;* orcid.org/0000-0001-6753-2800; Phone: 040-2301-7086; Email: svanjari@ee.iith.ac.in

Authors

Rahul Gangwar − *Department of Electrical Engineering, Indian Institute of Technology Hyderabad, Hyderabad 502284, India;* orcid.org/0000-0003-3391-4362

Debjyoti Ray − *Department of Chemistry, Indian Institute of Technology Hyderabad, Hyderabad 502284, India; Department of Chemistry, The Chinese University of Hong Kong, Shatin, NT 00000 Hong Kong SAR, China*

Karri Trinadha Rao − *Department of Electrical Engineering, Indian Institute of Technology Hyderabad, Hyderabad 502284, India*

Sajmina Khatun − *Department of Biomedical Engineering, Indian Institute of Technology Hyderabad, Hyderabad 502284, India*

Challapalli Subrahmanyam − *Department of Chemistry, Indian Institute of Technology Hyderabad, Hyderabad 502284, India*

Aravind Kumar Rengan − *Department of Biomedical Engineering, Indian Institute of Technology Hyderabad, Hyderabad 502284, India;* orcid.org/0000-0003-3994-6760

Complete contact information is available at: https://pubs.acs.org/10.1021/acsomega.2c01802

Notes

The authors declare no competing financial interest.

https://doi.org/10.1021/acsomega.2c01802
ACS Omega 2022, 7, 21025−21034

■ ACKNOWLEDGMENTS

The authors acknowledge the DST (Project No. DST/NM/NT/2021/01-1C), Ministry of Science & Technology, India, for funding the research.

■ REFERENCES

(1) Chakraborty, M.; Hashmi, M. S. J.An Overview of Biosensors and Devices. In *Encyclopedia of Smart Materials*; Elsevier, 2017; pp 1−24, DOI: 10.1016/b978-0-12-803581-8.10316-9.
(2) Ramasamy, R.; Gopal, N.; Kuzhandaivelu, V.; Murugaiyan, S. Biosensors in Clinical Chemistry: An Overview. *Adv. Biomed. Res.* **2014**, *3*, No. 67.
(3) Ali, J.; Najeeb, J.; Asim Ali, M.; Farhan Aslam, M.; Raza, A. Biosensors: Their Fundamentals, Designs, Types and Most Recent Impactful Applications: A Review. *J. Biosens. Bioelectron.* **2017**, *08*, 1−9.
(4) Vigneshvar, S.; Sudhakumari, C. C.; Senthilkumaran, B.; Prakash, H. Recent Advances in Biosensor Technology for Potential Applications - an Overview. *Front. Bioeng. Biotechnol.* **2016**, *4*, No. 11.
(5) The, D. R.; Toth, K.; Durst, R. A.; Wilson, G. S. Electrochemical biosensors: recommended definitions and classification1International Union of Pure and Applied Chemistry: Physical Chemistry Division, Commission I.7 (Biophysical Chemistry); Analytical Chemistry Division, Commission V.5 (Electroanalytical Chemistry).1. *Biosens. Bioelectron.* **2001**, *16*, 121−131.
(6) Gangwar, R.; Subrahmanyam, C.; Vanjari, S. R. K. Facile, Label-Free, Non-Enzymatic Electrochemical Nanobiosensor Platform as a Significant Step towards Continuous Glucose Monitoring. *ChemistrySelect* **2021**, *6*, 11086−11094.
(7) German, N.; Ramanaviciene, A.; Voronovic, J.; Ramanavicius, A. Glucose Biosensor Based on Graphite Electrodes Modified with Glucose Oxidase and Colloidal Gold Nanoparticles. *Microchim. Acta* **2010**, *168*, 221−229.
(8) Jiménez-Fiérrez, F.; González-Sánchez, M. I.; Jiménez-Pérez, R.; Iniesta, J.; Valero, E. Glucose Biosensor Based on Disposable Activated Carbon Electrodes Modified with Platinum Nanoparticles Electrodeposited on Poly(Azure A). *Sensors* **2020**, *20*, No. 4489.
(9) Gergeroglu, H.; Yildirim, S.; Ebeoglugil, M. F. Nano-Carbons in Biosensor Applications: An Overview of Carbon Nanotubes (CNTs) and Fullerenes (C60). *SN Appl. Sci.* **2020**, *2*, No. 603.
(10) Yáñez-Sedeño, P.; Campuzano, S.; Pingarrón, J. Fullerenes in Electrochemical Catalytic and Affinity Biosensing: A Review. *C* **2017**, *3*, No. 21.
(11) Casanova, A.; Iniesta, J.; Gomis-Berenguer, A. Recent Progress in the Development of Porous Carbon-Based Electrodes for Sensing Applications. *Analyst* **2022**, *147*, 767−783.
(12) Wen, Z.; Li, J. Hierarchically Structured Carbon Nanocomposites as Electrode Materials for Electrochemical Energy Storage, Conversion and Biosensor Systems. *J. Mater. Chem.* **2009**, *19*, 8707−8713.
(13) Cardenas-benitez, B.; Djordjevic, I.; Hosseini, S.; Martinez-chapa, S. O.; Madou, M. J. Review — Covalent Functionalization of Carbon Nanomaterials for Biosensor Applications: An Update. *J. Electrochem. Soc.* **2018**, *165*, B103−B117.
(14) Hwang, H. S.; Jeong, J. W.; Kim, Y. A.; Chang, M. Carbon Nanomaterials as Versatile Platforms for Biosensing Applications. *Micromachines* **2020**, *11*, No. 814.
(15) Saka, C. Overview on the Surface Functionalization Mechanism and Determination of Surface Functional Groups of Plasma Treated Carbon Nanotubes. *Crit. Rev. Anal. Chem.* **2018**, *48*, 1−14.
(16) Valsesia, A.; Ceccone, G.; Colpo, P.; Gilliland, D.; Ceriotti, L.; Hasiwa, M.; Rossi, F. Surface Functionalization and Patterning Techniques to Design Interfaces for Biomedical and Biosensor Applications. *Plasma Processes Polym.* **2006**, *3*, 443−455.
(17) Yüce, M.; Kurt, H. How to Make Nanobiosensors: Surface Modification and Characterisation of Nanomaterials for Biosensing Applications. *RSC Adv.* **2017**, *7*, 49386−49403.
(18) Kim, J. H.; Jin, J.; Lee, J.; Park, E. J.; Min, N. K. Covalent Attachment of Biomacromolecules to Plasma-Patterned and Functionalized Carbon Nanotube-Based Devices for Electrochemical Biosensing. *Bioconjugate Chem.* **2012**, *23*, 2078−2086.
(19) Sonawane, M. D.; Nimse, S. B. Surface Modification Chemistries of Materials Used in Diagnostic Platforms with Biomolecules. *J. Chem.* **2016**, *2016*, 1−19.
(20) Laurano, R.; Boffito, M.; Torchio, A.; Cassino, C.; Chiono, V.; Ciardelli, G. Plasma Treatment of Polymer Powder as an Eective Tool to Functionalize Polymers: Case Study Application on an Amphiphilic Polyurethane. *Polymers* **2019**, *11*, No. 2109.
(21) Nayak, L.; Rahaman, M.; Giri, R. Surface Modification/Functionalization of Carbon Materials by Different Techniques: An Overview. In *Springer Series on Polymer and Composite Materials*; Springer: Singapore, 2019; pp 65−98, DOI: 10.1007/978-981-13-2688-2_2.
(22) Baranov, O.; Levchenko, I.; Bell, J. M.; Lim, J. W. M.; Huang, S.; Xu, L.; Wang, B.; Aussems, D. U. B.; Xu, S.; Bazaka, K. From Nanometre to Millimetre: A Range of Capabilities for Plasma-Enabled Surface Functionalization and Nanostructuring. *Mater. Horiz.* **2018**, *5*, 765−798.
(23) Desmet, T.; Morent, R.; De Geyter, N.; Leys, C.; Schacht, E.; Dubruel, P. Nonthermal Plasma Technology as a Versatile Strategy for Polymeric Biomaterials Surface Modification: A Review. *Biomacromolecules* **2009**, *10*, 2351−2378.
(24) Kaushik, N. K.; Kaushik, N.; Linh, N. N.; Ghimire, B. Plasma and Nanomaterials: Fabrication and Biomedical Applications. *Nanomaterials* **2019**, *9*, 1−98.
(25) Joung, C. K.; Kim, H. N.; Lim, M. C.; Jeon, T. J.; Kim, H. Y.; Kim, Y. R. A Nanoporous Membrane-Based Impedimetric Immunosensor for Label-Free Detection of Pathogenic Bacteria in Whole Milk. *Biosens. Bioelectron.* **2013**, *44*, 210−215.
(26) Li, Y.; Cheng, P.; Gong, J.; Fang, L.; Deng, J.; Liang, W.; Zheng, J. Amperometric Immunosensor for the Detection of *Escherichia coli* O157: H7 in Food Specimens. *Anal. Biochem.* **2012**, *421*, 227−233.
(27) Xu, M.; Wang, R.; Li, Y. Electrochemical Biosensors for Rapid Detection of *Escherichia coli* O157:H7. *Talanta* **2017**, *162*, 511−522.
(28) Barreiros dos Santos, M.; Agusil, J. P.; Prieto-Simón, B.; Sporer, C.; Teixeira, V.; Samitier, J. Highly Sensitive Detection of Pathogen *Escherichia coli* O157: H7 by Electrochemical Impedance Spectroscopy. *Biosens. Bioelectron.* **2013**, *45*, 174−180.
(29) Sundaresan, V.; Do, H.; Shrout, J. D.; Bohn, P. W. Electrochemical and Spectroelectrochemical Characterization of Bacteria and Bacterial Systems. *Analyst* **2021**, *147*, 22−34.
(30) Yu, D.; Li, R.; Sun, X.; Zhang, H.; Yu, H.; Dong, S. Colorimetric and Electrochemical Dual-Signal Method for Water Toxicity Detection Based on *Escherichia coli* and p-Benzoquinone. *ACS Sens.* **2021**, *6*, 2674−2681.
(31) Bi, L.; Wang, X.; Cao, X.; Liu, L.; Bai, C.; Zheng, Q.; Choo, J.; Chen, L. SERS-Active Au@Ag Core-Shell Nanorod (Au@AgNR) Tags for Ultrasensitive Bacteria Detection and Antibiotic-Susceptibility Testing. *Talanta* **2020**, *220*, No. 121397.
(32) Lin, D.; Li, B.; Qi, J.; Ji, X.; Yang, S.; Wang, W.; Chen, L. Low Cost Fabrication of Microfluidic Paper-Based Analytical Devices with Water-Based Polyurethane Acrylate and Their Application for Bacterial Detection. *Sens. Actuators, B* **2020**, *303*, No. 127213.
(33) Zhong, M.; Yang, L.; Yang, H.; Cheng, C.; Deng, W.; Tan, Y.; Xie, Q.; Yao, S. An Electrochemical Immunobiosensor for Ultrasensitive Detection of *Escherichia coli* O157:H7 Using CdS Quantum Dots-Encapsulated Metal-Organic Frameworks as Signal-Amplifying Tags. *Biosens. Bioelectron.* **2019**, *126*, 493−500.
(34) Wang, H.; Fan, Y.; Yang, Q.; Sun, X.; Liu, H.; Chen, W.; Aziz, A.; Wang, S. Boosting the Electrochemical Performance of PI-5-CA/C-SWCNT Nanohybrid for Sensitive Detection of *E. coli* O157:H7 From the Real Sample. *Front. Chem.* **2022**, *10*, No. 843859.
(35) Ray, D.; Chawdhury, P.; Bhargavi, K. V. S. S.; Thatikonda, S.; Lingaiah, N.; Subrahmanyam, C. Ni and Cu Oxide Supported γ-Al2O3packed DBD Plasma Reactor for CO2activation. *J. CO2 Util.* **2021**, *44*, No. 101400.

https://doi.org/10.1021/acsomega.2c01802
ACS Omega 2022, 7, 21025−21034

(36) Haye, E.; Job, N.; Wang, Y.; Penninckx, S.; Stergiopoulos, V.; Tumanov, N.; Cardinal, M.; Busby, Y.; Colomer, J.; Su, B.; Pireaux, J.; Houssiau, L. Journal of Colloid and Interface Science ZnO / Carbon Xerogel Photocatalysts by Low-Pressure Plasma Treatment, the Role of the Carbon Substrate and Its Plasma Functionalization. *J. Colloid Interface Sci.* **2020**, *570*, 312−321.
(37) Subrahmanyam, C.; Bulushev, D. A.; Kiwi-Minsker, L. Dynamic Behaviour of Activated Carbon Catalysts during Ozone Decomposition at Room Temperature. *Appl. Catal., B* **2005**, *61*, 98−106.

https://doi.org/10.1021/acsomega.2c01802
ACS Omega 2022, 7, 21025−21034